Sample covariance based estimation of Capon algorithm error probabilities

Sample Covariance Based Estimation of Capon Algorithm Error Probabilities

Christ D. Richmond*,[1] and Robert L. Geddes*
[1]*Senior Member, IEEE*
{christ,geddes}@ll.mit.edu

Ramis Movassagh† and Alan Edelman†
Dept. Mathematics, MIT
Cambridge, MA 02139
{ramis,edelman}@math.mit.edu

***Abstract*— The method of interval estimation (MIE) provides a strategy for mean squared error (MSE) prediction of algorithm performance at low signal-to-noise ratios (SNR) below estimation threshold where asymptotic predictions fail. MIE interval error probabilities for the Capon algorithm are known and depend on the true data covariance and assumed signal array response. Herein estimation of these error probabilities is considered to improve representative measurement errors for parameter estimates obtained in low SNR scenarios, as this may improve overall target tracking performance. A statistical analysis of Capon error probability estimation based on the data sample covariance matrix is explored herein.**

I. Introduction

Recent analysis of a maximum a posteriori penalty function (MAP-PF) based tracker demonstrates the benefit of using the Cramér-Rao bound (CRB) to represent the measurement error in bearing estimates [1]. Low SNR, however, renders the CRB an inadequate representation of measurement error resulting in poorer performance of the tracking algorithm [2]. As an example, Figure 1 shows the root mean squared error (RMSE) performance of a bearing only Kalman filter (KF) that received bearing measurements [from maximum-likelihood (ML)] under low SNR conditions, but used the CRB to represent their MSE. The KF predicts an RMSE that is more optimistic than the actual RMSE realized by the tracker. The goal herein is to use an improved measure of MSE for low SNR scenarios as a means to (i) reduce the realized RMSE of the KF, (ii) improve the tightness of KF prediction of RMSE, and (iii) to make KF prediction more conservative in the low SNR regime.

The method of interval estimation (MIE) is a technique for extending asymptotic/high SNR predictions like the CRB to lower SNR scenarios [3], [4]. MIE discretizes the integral for mean squared error (MSE) based on the structure of the underlying ambiguity function for parameter estimation. The parameter estimate $\widehat{\theta}$ of the true parameter θ_1, for example, has MSE approximated by

$$E\left\{(\widehat{\theta}-\theta_1)^2\right\} \simeq \left[1-\sum_{m=2}^{M} P_e(\widehat{\theta}=\theta_m|\theta_1)\right]\sigma^2_{ASYMP}(\theta_1) + \sum_{m=2}^{M} P_e(\widehat{\theta}=\theta_m|\theta_1)(\theta_m-\theta_1)^2 \quad (1)$$

where $\sigma^2_{ASYMP}(\theta_1)$ is the asymptotic MSE (e.g. based on the CRB or Taylor's theorem), and $P_e(\widehat{\theta}=\theta_m|\theta_1)$ is the error probability, providing a measure of the likelihood of the parameter estimation algorithm choosing an estimate due to a peak at θ_m when the true parameter value is θ_1. Ultimately it is desired to explore the improvement in tracking performance MIE might provide for low SNR cases. The important enabler for MIE is the interval error probability $P_e(\widehat{\theta}=\theta_m|\theta_1)$ that identifies the boundary between the high SNR / asymptotic region of performance and the low SNR region.

In practice one must rely on some data based estimate of the error probability, as well as a data based estimate of the asymptotic MSE. The goal of this paper is to assess the statistical properties of a sample covariance based (SCB) estimate of the Capon interval error probabilities. This will allow quantification of the reliability of such an approach, including e.g. how the number data samples affects the fidelity of these probability estimates and what strategies are best for such practical estimation.

II. Statistics for SCB Estimate of Capon Algorithm Error Probabilities

Reference [4] provides the details of applying MIE to the Capon algorithm [5]. Let the signal at angle θ have array response $\mathbf{v}(\theta)$ for an N sensor array; let the true data covariance be $\mathbf{R}$ and sample covariance matrix (SCM) obtained from L data observations be denoted $\widehat{\mathbf{R}}$. Consider the Capon algorithm evaluated at point θ:

$$P_{Capon}(\theta) = \frac{1}{L-N+1}\cdot\frac{1}{\mathbf{v}^H(\theta)\widehat{\mathbf{R}}^{-1}\mathbf{v}(\theta)}. \quad (2)$$

The two-point error probability facilitating application of MIE is given by

$$P_e^{Capon}(\theta_a|\theta_b) \triangleq \Pr\left[P_{Capon}(\theta_a) > P_{Capon}(\theta_b)\right]. \quad (3)$$

*The authors currently work for MIT Lincoln Laboratory. Opinions, interpretations, conclusions, and recommendations are those of the authors and are not necessarily endorsed by the United States Government.

†This work was sponsored by the National Science Foundation under grants CCF-0829421 and DMS-1035400.

Define parameters $P_+(F), P_-(F)$, and $I_{ab}(F)$ such that:

$$P_{\pm}(F) \triangleq \frac{\mathbf{v}^H(\theta_b)\mathbf{R}^{-1}\mathbf{v}(\theta_b) \pm F\mathbf{v}^H(\theta_a)\mathbf{R}^{-1}\mathbf{v}(\theta_a)}{2} \quad \text{and} \quad I_{ab}(F) \triangleq F\left|\mathbf{v}^H(\theta_a)\mathbf{R}^{-1}\mathbf{v}(\theta_b)\right|^2; \tag{4}$$

and also define $\lambda_{\pm}(F)$, $l_\lambda(F)$, and $\mathcal{S}_\lambda(F)$:

$$\lambda_{\pm}(F) = P_-(F) \pm \sqrt{P_+^2(F) - I_{ab}(F)}, \quad l_\lambda(F) \triangleq -\frac{\lambda_+(F)}{\lambda_-(F)}, \quad \mathcal{S}_\lambda(F) \triangleq \text{sign}\left[\lambda_-(F)\right]. \tag{5}$$

It can be shown that the exact pairwise error probability for the Capon algorithm is given by [4]

$$P_e^{Capon}(\theta_a|\theta_b) = 0.5 \cdot \{1 + \mathcal{S}_\lambda(1)\} - \mathcal{S}_\lambda(1) \cdot \mathcal{F}[l_\lambda(1), L - N + 2] \tag{6}$$

where $\mathcal{F}(x, J)$ is the cumulative distribution function (cdf) for a special case of the complex central F statistic:

$$\mathcal{F}(x, J) \triangleq \frac{x^J}{(1+x)^{2J-1}} \sum_{k=0}^{J-1} \left(\begin{array}{c} 2J-1 \\ k+J \end{array} \right) \cdot x^k. \tag{7}$$

While eq(6) is exact, it is somewhat challenging to analyze a data based estimate of this probability. Ignoring the apparent statistical dependence between the two points $P_{Capon}(\theta)$, $\theta = \theta_a, \theta_b$, however, yields a simple approximation of the error probability that is surprisingly accurate in many scenarios:

$$\begin{aligned} &\Pr\left[P_{Capon}(\theta_a) > P_{Capon}(\theta_b)\right] \simeq \\ &\Pr\left[\frac{{}_a\chi^2_{L-N+1}}{{}_b\chi^2_{L-N+1}} > \frac{\mathbf{v}^H(\theta_a)\mathbf{R}^{-1}\mathbf{v}(\theta_a)}{\mathbf{v}^H(\theta_b)\mathbf{R}^{-1}\mathbf{v}(\theta_b)}\right] \\ &= \mathcal{F}\left[\frac{\mathbf{v}^H(\theta_a)\mathbf{R}^{-1}\mathbf{v}(\theta_a)}{\mathbf{v}^H(\theta_b)\mathbf{R}^{-1}\mathbf{v}(\theta_b)}, L - N + 1\right] \\ &\triangleq P_{\tilde{e}}^{Capon}(\theta_a|\theta_b). \end{aligned} \tag{8}$$

The assumed independence of points θ_a, θ_b allows use of the Capon-Goodman result [6], leading to a ratio of independent chi-squared random variables that is known to be F-distributed. Note that (8) is parameterized by a ratio of Capon spectral points θ_a, θ_b. Define the ratio of SCB Capon spectral estimates as the following random variable:

$$F_\Delta \triangleq \frac{\mathbf{v}^H(\theta_a)\widehat{\mathbf{R}}^{-1}\mathbf{v}(\theta_a)}{\mathbf{v}^H(\theta_b)\widehat{\mathbf{R}}^{-1}\mathbf{v}(\theta_b)}. \tag{9}$$

The goal of this paper is first to assess the statistical properties of the following SCB estimator of the Capon error probability:

$$\widehat{P}_{\tilde{e}}^{Capon}(\theta_a|\theta_b, F_\Delta) = \mathcal{F}\left[F_\Delta, L - N + 1\right] \tag{10}$$

and second to begin discussion of initial results for the statistical analysis of a SCB estimate of the exact two-point probability found in [4]. The pdf of F_Δ is derived in [4] and includes the affects of statistical dependence between points θ_a, θ_b. Thus, the desired moments of $\widehat{P}_{\tilde{e}}^{Capon}(\theta_a|\theta_b, F_\Delta)$ can be obtained via numerical integration:

$$E\left\{\left[\widehat{P}_{\tilde{e}}^{Capon}(\theta_a|\theta_b, F_\Delta)\right]^M\right\} = \int_0^\infty P_{F_\Delta}(F)\left[\widehat{P}_{\tilde{e}}^{Capon}(\theta_a|\theta_b, F)\right]^M dF. \tag{11}$$

The exact probability density function for $\widehat{P}_{\tilde{e}}^{Capon}(\theta_a|\theta_b, F_\Delta)$ can likewise be deduced with some additional effort.

Regarding (6), define the $N \times 2$ matrix $\mathbf{V} = [\mathbf{v}(\theta_a)|\mathbf{v}(\theta_b)]$. One can estimate $\lambda_{\pm}(F)$ and $l_\lambda(F)$ via the eigenvalues of the 2×2 matrix

$$\widehat{\lambda}_{\pm}(F) = \lambda_{1,2}\left\{\left[\begin{array}{cc} -F & 0 \\ 0 & 1 \end{array}\right](\mathbf{V}^H\widehat{\mathbf{R}}^{-1}\mathbf{V})^{-1}\right\}. \tag{12}$$

Since results apply regardless of how $l_\lambda(F)$ is formed, the condition number of (12) is chosen for convenience:

$$\widehat{l}_\lambda(F) \triangleq -\frac{\arg\max_{\widehat{\lambda}_-, \widehat{\lambda}_+} |\widehat{\lambda}(F)|}{\arg\min_{\widehat{\lambda}_-, \widehat{\lambda}_+} |\widehat{\lambda}(F)|} \tag{13}$$

Let $K = L - N + 2$; It can be shown that its pdf is given exactly by

$$\widehat{l}_\lambda \sim c \cdot \frac{(l+1)l^{K-2}}{(a_1 - la_2)^{2K-1}}\left[1 + \left(\frac{a_1 - la_2}{la_1 - a_2}\right)^{2K-1}\right] \tag{14}$$

$l \geq 0$ where the constants a_1 and a_2 are determined from $\mathbf{R}, \mathbf{V}$ and F; also where sign(a_2) = $-$sign(a_1) and the normalizing constant is given by

$$c = \frac{2^{2(K-1)}(-a_1a_2)^K\Gamma(K - \frac{1}{2})\Gamma(2K-1)}{\sqrt{\pi}\Gamma(K-1)(a_1 - a_2)}. \tag{15}$$

This paper will focus on the error probability estimator in eq(10) given its relative simplicity. Analysis of a SCB estimate of eq(6) will be the subject of future analysis.

III. Numerical Examples

A. Statistics for Estimated Capon Error Probabilities

Using eq(11) one can explore the fidelity of using a SCB approach to estimating error probabilities for the Capon algorithm. Consider a bearing estimation scenario involving a single planewave source and a set of signal bearing snapshots $\mathbf{x}(l) \sim \mathcal{CN}[\mathbf{0}, \mathbf{I} + \sigma_S^2\mathbf{v}(\theta_T)\mathbf{v}^H(\theta_T)]$, $l = 1, 2, \ldots, L$, for an $N = 18$ element uniform linear array (ULA) with slightly less than $\lambda/2$ element spacing. The array has a 3dB beamwidth of 7.2 degrees and the desired target signal is arbitrarily placed at $\theta_T = 90$ degrees (array broadside). The signal parameter search space of interest is defined to be $\theta \in [60^\circ, 120^\circ]$. Figure 2 illustrates the Capon error probability for the peak sidelobe as a function of element level SNR for $L = 1.5N, 3N$, and $6N$. Note that the approximation in eq(8) is illustrated by the blue circle curves and is very accurate as it falls nearly right on top of the exact error probability in eq(6)

illustrated by the solid blue curve. The mean of the SCB estimate $\widehat{P}_{\tilde{e}}^{Capon}(\theta_a|\theta_b, F_\Delta)$ is illustrated by the red curve and its standard deviation by the black dashed curves. Clearly, a small bias persists even with increasing sample support L. Analysis shows that this bias is the result of a SNR loss due to reliance on an estimated covariance matrix. Surprisingly the value of this bias is very weakly dependent on array size N and sample support L. It is approximately $\sim$2dB for many cases. When one corrects for this bias, a much better fit of the statistics for $\widehat{P}_{\tilde{e}}^{Capon}(\theta_a|\theta_b, F_\Delta)$ to the true value is obtained. This improved fit is illustrated in the lower right image of Figure 2 for the $L = 3N$ case. The KF generates an estimate of the signal power level σ_S^2 [2] that can be used to help apply this correction in practice. It is also noteworthy that the variance of the SCB estimates of probability decrease with increasing SNR and increasing sample support L. Consequently, one can expect increasing accuracy as the SNR increases toward the threshold SNR.

B. Framework for Kalman Filter Sensitivity Analysis

How does the KF perform if the error bars (MSE estimate) for the bearing measurements are optimistically small but the bearing measurement is rather erroneous? One can explore the sensitivity of the KF for varied levels of accuracy for the MSE estimates it's given for the bearing measurements via simulation. Figure 3 illustrates via a block diagram the framework for the KF analysis via simulation. First a target bearing trajectory is generated based on a Markov model for the bearing rate. Simulated array data can then be generated based on this trajectory using one's choice of target fluctuation models. The Capon algorithm (or other, e.g. ML) can then be applied to generate bearing estimates over time that can be subsequently fed into the KF. One can then examine the resulting RMSE of the KF as one varies the accuracy of the MSE estimates that accompany the bearing measurements fed to the KF.

The state vector within the Kalman filter is a three state system composed of: target bearing, target bearing rate and target received power. The target bearing rate is assumed to have the form of a first order Markov random variable, while the target received power is modeled as a random bias. The target bearing is just the integral of the bearing rate. These states are first represented in the form of a set of continuous stochastic differential equations that are easily transformed into a discrete set of difference equations [8].

The actual true target trajectory is generated as a single realization of this same model for target bearing and bearing rate. An example is shown in Figure 3. The two parameters for the first order Markov for target bearing rate are the time constant defined to be 1200 seconds, and the standard deviation of the target bearing rate which is 3.5e-3 (deg/sec). The time step is one second and the duration of the simulation is 500 time steps. Measurements are processed at each time step. The variance assigned to each measured Capon bearing estimate is assigned either an asymptotic value based on the Taylor series [7] (accounting for local errors) or a non-asymptotic value based on MIE and defined by equation (1) (accounting for both local and global errors).

The Kalman filter is run 5000 times, each time producing a filtered target bearing and bearing rate which are compared to the true trajectory to obtain average errors. The sample error covariance from the 5000 Monte Carlo trials is compared to the Kalman filters own predicted error covariance.

C. Kalman Filter RMSE Performance

Herein a simple $N = 18$ element horizontal line array that measures data from a distant target near array broadside is considered. The target bearing trajectory used for simulation is shown in Figure 3. The bearing estimates are obtained via the Capon algorithm where each estimate uses $L = 2N$ training samples in the covariance estimate. Figure 4 illustrates the resulting RMSE performance of the KF for varied SNR levels. The threshold SNR (element level) for this simulation is ~ -8dB. The first plot in Figure 4 shows the KF RMSE when the signal level is above threshold SNR. While only visible in the other images there are four curves shown. The solid curves show the true bearing RMSE realized by the KF and the dashed lines show the KF's prediction of the bearing RMSE. The red lines are obtained when the MSE estimates accompanying the Capon bearing estimates derive from Taylor series [7] (asymptotic), and the blue lines are obtained when the MSE estimates derive from MIE (non-asymptotic). The second and third images in Figure 4 shows the performance when the signal level falls below threshold. It is noteworthy that for these low SNR signals the true KF bearing RMSE has been reduced by using MIE and that the tightness of fit between the true RMSE and the KF predicted RMSE improves significantly. Lastly, use of MIE results in a KF predicted error that is more conservative at low SNRs as desired.

IV. Conclusions

This paper explores the notion of using MIE to improve the accuracy of MSE estimates attached to bearing measurements fed to a Kalman filter (KF) tracker. MIE requires calculation of error probabilities; therefore, a simple SCB estimate of these probabilities was proposed and analyzed. It was found that an SNR loss of $\sim$2dB was present and nearly invariant to array size N and sample support L. Correcting for this bias was shown to significantly improve the match between the statistics of these estimated error probabilities and the true values. It was also shown that the accuracy of these SCB error probability estimate improves with SNR and sample support, getting better as one approaches the threshold SNR from below. A simulation framework was exploited to assess the benefit of improved MSE estimates to the KF overall performance. It is shown that for low SNR signals the true KF bearing RMSE is reduced by using MIE and that the tightness of fit between the true RMSE and the KF predicted RMSE improves significantly. Use of MIE also results in a more conservative prediction of error variance by the KF.

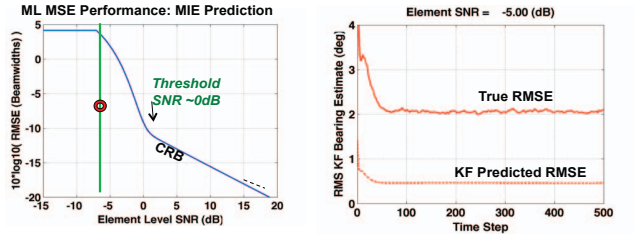

Fig. 1. Kalman filter performance: Below threshold SNR bearing estimates, but CRB used to represent MSE

Future work will further explore the practicalities of such an approach, as well as consideration of more dynamic target trajectories with larger variations in SNR levels.

ACKNOWLEDGEMENTS

The authors would like to thank Dr. Kristine Bell for useful discussions on tracking and for providing MATLAB scripts for the MAP-PF tracker. We would also like to thank the National Science Foundation for support through grant CCF-0829421 and for support through grant DMS-1035400.

REFERENCES

[1] K. L. Bell, R. E. Zarnich, R. Wasyk, "MAP-PF Wideband Multitarget and Colored Noise Tracking," *Proceedings of the ICASSP*, Dallas, Texas, March 2010.

[2] K. L. Bell, H. L. Van Trees, "Posterior Cramér-Rao Bound for Tracking Target Bearing," *Proceedings of the Adaptive Sensor and Array Processing Workshop*, MIT Lincoln Laboratory, 2005.

[3] H. L. Van Trees and K. L. Bell, Eds., *Bayesian Bounds for Parameter Estimation and Nonlinear Filtering/Tracking*. New York:Wiley, 2007.

[4] C. D. Richmond, "Capon Algorithm Mean Squared Error Threshold SNR Prediction and Probability of Resolution," *IEEE Transactions on Signal Processing*, Vol. 53, No. 8, pp. 2748-2764, Aug. 2005.

[5] J. Capon, "High–Resolution Frequency–Wavenumber Spectrum Analysis," *Proceedings of the IEEE*, Vol. 57, 1408–1418 (1969).

[6] J. Capon and N.R. Goodman,"Probability Distributions for Estimators of Frequency Wavenumber Spectrum," *Proceedings of the IEEE*, Vol. 58, No. 10, 1785–1786 (1970).

[7] C. Vaidyanathan, K. M. Buckley, "Performance Analysis of the MVDR Spatial Spectral Estimator," *IEEE Transactions on Signal Processing*, Vol. 43, No. 6, pp. 1427–1437, June 1995.

[8] A. Gelb, Editor, *Applied Optimal Estimation*, MIT Press, 1989.

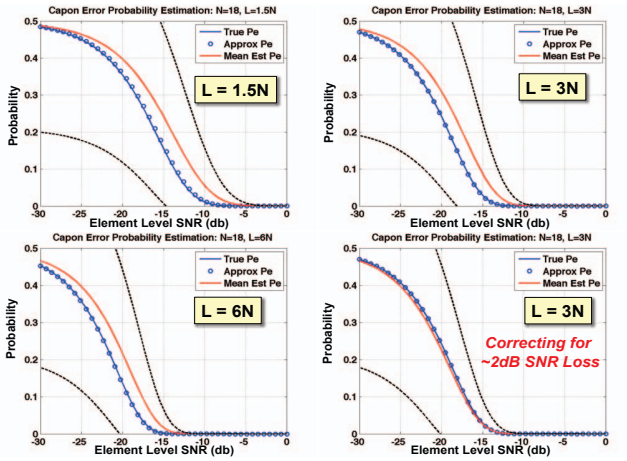

Fig. 2. Statistics of $\widehat{P}_{\tilde{e}}^{Capon}(\theta_a|\theta_b, F_\Delta)$ for θ_a of peak sidelobe: $N = 18$ element ULA

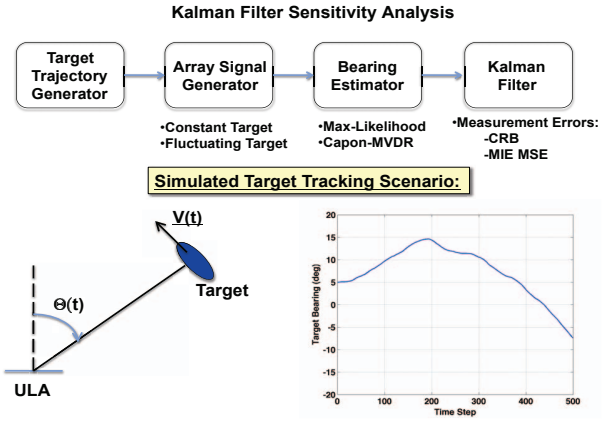

Fig. 3. Kalman filter sensitivity analysis framework

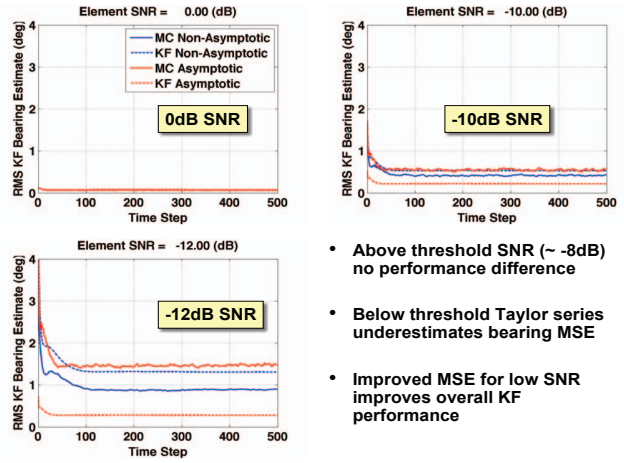

Fig. 4. Kalman filter realized MSE Performance: Capon algorithm bearing measurements as input